BIOCHIMICA ET BIOPHYSICA ACTA
BBA

Optical detection of membrane dipole potential: avoidance of fluidity and dye-induced effects

Ronald J. Clarke *, David J. Kane

Department of Biophysical Chemistry, Max-Planck-Institut für Biophysik, Kennedyallee 70, D-60596 Frankfurt am Main, Germany

Received 19 July 1996; revised 12 September 1996; accepted 12 September 1996

Abstract

Fluorescent styrylpyridinium dyes have recently been suggested as probes of the membrane dipole potential and of the kinetics of electrogenic ion pumps. It is necessary, however, to be able to confidently attribute observed fluorescence changes to electrical effects alone and avoid interference from changes in membrane fluidity. Furthermore, the effect of the dyes themselves on the dipole potential must be investigated. The effect of membrane fluidity on the fluorescence excitation and emission spectra of the dyes RH421 and di-8-ANEPPS have been investigated in lipid vesicles by temperature scans between 15 and 60°C. Both dyes show significant temperature-dependent shifts of their excitation spectra, the magnitude of which depend on the emission wavelength and on the lipid structure. In order to eliminate membrane fluidity effects, fluorescence must be detected at the red edge of the emission spectrum; in this case 670 nm. In order to avoid dye-induced shifts of the excitation spectra of membrane-bound dye, an excess molar ratio of lipid to dye of at least 200-fold is necessary. Fluorescence ratio measurements indicate qualitatively that dimyristoylphosphatidylcholine has a significantly higher dipole potential than that of dioleoylphosphatidylcholine.

Keywords: Voltage sensitive dye; Dipole potential; Lipid vesicle; Viscosity; Excited state relaxation; Na^+,K^+-ATPase

1. Introduction

Potential-sensitive fluorescent styryl dyes, such as RH421, RH160 and di-4- and di-8-ANEPPS, originally developed in the laboratories of Grinvald [1,2] and Loew [3–5], are presently attracting great interest as a means of optical imaging of electrical transients in neurons [6–9] and for the investigation of the reaction mechanisms of ion pumps, e.g., the Na^+,K^+-ATPase [10–14]. The dyes respond to a change in transmembrane potential with a shift in their fluorescence excitation spectrum. In addition to their response to transmembrane potential it has been found that the dyes are very sensitive to local electric fields which arise from charges within the membrane [9,15–17]. This has led to the proposal that the dyes might be used as probes of the membrane dipole potential [18,19].

A quantitative determination of local electric field strength due to either transmembrane potential or dipole potential using styryl dyes is made difficult because of the strong dependence of the fluorescence intensity on the

* Corresponding author. Fax: +49 (69) 6303305; e-mail: clarker@kennedy.mpibp.uni-frankfurt.de.

PII S0005-2736(96)00188-5

dye's environment. Montana et al. [20] have suggested that this problem can be overcome by dual wavelength excitation ratiometric fluorescence measurements, similar to the method often employed when measuring cellular Ca^{2+} concentrations with the fluorescent indicator fura-2 [21]. This method has since been applied to electrical measurements using styryl dyes in a variety of cell and model membrane preparations [18,22–25]. It is able to circumvent artifactual variations in fluorescence intensity due to small variations in the total membrane-bound dye concentration. When using the dyes as probes of electrical events in cells or model membrane systems, however, it is of critical importance to rule out any other possible causes of changes of the fluorescence ratio, e.g., changes in membrane fluidity or the conformation of membrane proteins. Furthermore, contributions of the dyes themselves to the magnitude of the membrane potential or the dipole potential must be excluded.

Time-resolved fluorescence intensity and anisotropy measurements of the styryl dye RH421 [25,26] have shown that the dye undergoes an excited-state reaction involving a conformational change of the dye molecular structure and a simultaneous reorganization of the solvent shell. The timescale of the excited state reaction is of the order of 0.1 ns [25], which is less than an order of magnitude faster than the average lifetime of the short-wavelength fluorescence emission of dye associated to dimyristoylphosphatidylcholine (DMPC) vesicles of 0.6 ns [17]. Because the rates of the excited state reaction and fluorescence emission are not sufficiently separated, changes in the fluidity of the dye environment may cause shifts in the fluorescence excitation and emission spectra which are unrelated to any electrical phenomena. This could come about via an effect of membrane fluidity on the rate of the excited state reaction.

An effect of membrane fluidity on dye in the ground state is also conceivable. It has been found previously that both the fluorescence emission spectrum [13,15,27] and the quantum yield [25] of styryl dyes bound to lipid membranes depends on the excitation wavelength. This can be explained by different populations of dye, e.g. different orientations with respect to the membrane normal. Membrane fluidity is a factor which could reasonably influence the distribution of dye within the membrane and hence induce fluorescence changes.

Recently it was shown by Malkov and Sokolov [28] that the binding of some styryl dyes to planar lipid membranes leads to a significant acceleration of the transport of hydrophobic anions through the membrane. They interpreted this as being due to a dye-induced increase in the dipole potential. Therefore, it is reasonable to expect that increasing dye surface density in the membrane may induce sufficient changes in the dipole potential so that shifts in the fluorescence excitation spectrum of bound dye are observed. Conditions would then have to be found such that this effect can be minimized. This effect would be particularly significant if one is using the dyes to monitor the kinetics of ion pumps, e.g. the Na^+,K^+-ATPase, since it can be expected that the dye-induced changes to the dipole potential could significantly alter the rate constants of electrogenic reaction steps.

The purpose of the present paper is to investigate the effect of membrane fluidity and dye–dye interactions on the fluorescence and absorbance properties of the two dyes RH421 and di-8-ANEPPS (see Fig. 1). It will be

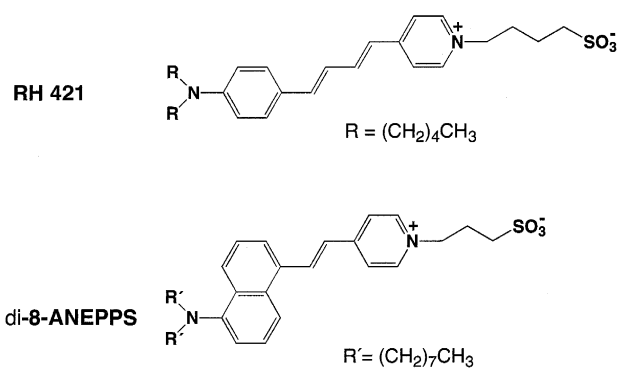

Fig. 1. Structures of RH421 and di-8-ANEPPS.

shown that the excitation ratiometric method of Montana et al. [20] does not always allow a distinction between electrical and fluidity changes. Conditions under which membrane fluidity has no influence will be described which enables fluorescence changes to be attributed to changes in electrical potential alone. Furthermore, the excess lipid to dye ratio necessary to avoid dye-induced changes to the dipole potential will be assessed.

2. Materials and methods

N-(4-Sulfobutyl)-4-(4-(*p*-(dipentylamino)phenyl)butadienyl)-pyridinium inner salt (RH421) and 4-(2-(6-(dioctylamino)-2-naphthalenyl)ethenyl)-1-(3-sulfopropyl)-pyridinium inner salt (di-8-ANEPPS) were obtained from Molecular Probes (Eugene, OR). In vesicles as well as in aqueous solution, both dyes showed a single long wavelength fluorescence emission band regardless of the excitation wavelength. A series of stock solutions of the dyes were prepared in ethanol. For spectral measurements, 5 μl of an ethanolic dye solution was added to 1 ml of aqueous solvent. The final solutions thus contained a small and constant percentage of 0.5% ethanol. In the case of experiments in the presence of lipid vesicles, after addition of the dye, 15 min equilibration time was left for RH421 and 1 h for di-8-ANEPPS to allow for dye disaggregation and incorporation into the membrane. Small volumes (≤ 10 μl) of phloretin or 6-ketocholestanol were also added from stock solutions in ethanol. The effect of the small volume of ethanol added on the absorbance or fluorescence spectra of membrane-bound dye was checked in separate control experiments and found to be negligible. The incorporation of phloretin into the vesicles is rapid, but in the case of 6-ketocholestanol it was necessary to equilibrate solutions overnight before making any measurements.

Dimyristoylphosphatidylcholine (DMPC), dioleoylphosphatidylcholine (DOPC) and egg phosphatidylcholine were obtained from Avanti Polar Lipids (Alabaster, AL). Unilamellar vesicles were prepared by the ethanol injection method described in detail elsewhere [19,25]. The final vesicle suspension contained no detectable trace of ethanol, i.e., [ethanol] ≤ 10 μM, according to a nicotinamide adenine dinucleotide/alcohol dehydrogenase enzymatic assay (Boehringer, Mannheim). Dialysis tubing was purchased from Medicell International (London, UK). The phospholipid content of the vesicle suspension was determined by the phospholipid B test from Wako (Neuss, Germany).

Measurements with the vesicles were performed in a buffer containing 30 mM Tris, 1 mM EDTA, and 150 mM NaCl. The pH of the buffer was adjusted to 7.2 with HCl. All solutions were prepared using deionised water. The origins of the various reagents used were as follows: Tris-[(hydroxymethyl)amino]methane (99.9%, Sigma Chemical Co., St. Louis, MO), EDTA (99%, Sigma), NaCl (analytical grade, Merck, Darmstadt, Germany), HCl (1.0 M Titrisol solution, Merck), ethanol (analytical grade, Merck), phloretin ($>$ 98%, Fluka, Buchs, Switzerland) and 6-ketocholestanol (Sigma).

The absorbance measurements were performed with an Hitachi (Tokyo, Japan) U-3000 spectrophotometer equipped with a head-on photomultiplier so as to minimize the effects of light scattering. Steady state fluorescence measurements were recorded with an Hitachi F-4500 fluorescence spectrophotometer. To minimize contributions from scattering of the exciting light and higher order wavelengths, glass cut-off filters were used in front of the excitation and emission monochromators where appropriate. The temperature of the cuvette holders was thermostatically controlled.

The association of substrates to lipid vesicles can often be analyzed according to a binding model [16,25,29]. The apparent microscopic binding constant, K, is defined according to the mass action law by

$$K = \frac{c^*_{XL}}{(nc^*_L - c^*_{XL})(c^*_X - c^*_{XL})} \quad (1)$$

where c^*_L, c^*_X, and c^*_{XL} represent the total concentrations of lipid, substrate (free and bound) and bound

substrate, respectively. n is the number of substrate binding sites per lipid molecule. Rearranging Eq. (1), the concentration of bound substrate molecules, c^*_{XL}, can be calculated as follows.

$$c^*_{XL} = \frac{1 + K(c^*_X + nc^*_L) - \left\{\left[1 + K(c^*_X + nc^*_L)\right]^2 - 4K^2 nc^*_L c^*_X\right\}^{1/2}}{2K} \tag{2}$$

In the case of phloretin as the substrate, a correction to Eqs. (1) and (2) must be made to allow for the presence of protonated (uncharged) and deprotonated (negatively charged) forms in the aqueous solution. Phloretin has a pK_a of 7.3 [30], so that at the pH used for the measurements, in the absence of vesicles approximately equal amounts of the protonated and deprotonated forms would be present. Le Fevre and Marshall [30] have shown, however, that it is the uncharged protonated form of phloretin that binds to red blood cell membranes. Furthermore, Andersen et al. [31] have found that the protonated form of phloretin is the active species in modifying the conductance of planar lipid bilayer membranes. Therefore, we assume here that only the protonated form of phloretin binds to the vesicle membrane. The concentration of protonated phloretin, c_{HX}, in the aqueous solution is then given by

$$c_{HX} = c^*_X - c^*_{XL} - c_X \tag{3}$$

where c_X is the concentration of free deprotonated phloretin. From the Henderson-Hasselbalch equation it can be shown that c_{HX} and c_X are related by

$$c_X = c_{HX} \cdot 10^{pH - pK_a} \tag{4}$$

Substitution of Eq. (4) for c_X into Eq. (3) leads on rearrangement to

$$c_{HX} = \frac{c^*_X - c^*_{XL}}{1 + 10^{pH - pK_a}} \tag{5}$$

Eq. (5) must now be inserted into the denominator of Eq. (1) in the place of $(c^*_X - c^*_{XL})$, so that the modified forms of Eqs. (1) and (2) with pH correction now become

$$K = \frac{c^*_{XL} \cdot (1 + 10^{pH - pK_a})}{(nc^*_L - c^*_{XL})(c^*_X - c^*_{XL})} \tag{6}$$

and

$$c^*_{XL} = \frac{1 + 10^{pH - pK_a} + K(c^*_X + nc^*_L) - \left\{\left[1 + 10^{pH - pK_a} + K(c^*_X + nc^*_L)\right]^2 - 4K^2 nc^*_L c^*_X\right\}^{1/2}}{2K} \tag{7}$$

The fluorescence excitation ratio, R, of dye in the membrane is assumed to be related to the concentration of bound substrate by

$$R = R_0 + (R - R_0) \cdot \frac{c^*_{XL}}{nc^*_L} \tag{8}$$

where R_0 is the ratio before the addition of substrate and R is the ratio when all the substrate binding sites are occupied. Substituting Eq. (2) or Eq. (7) (for phloretin) into Eq. (8) for c^*_{XL} and fitting the resulting equation to the fluorescence titration data of R as a function of the total substrate concentration (c^*_X) allows values of K and n to be determined. The non-linear least-squares fit was carried out using the commercially available program ENZFITTER.

3. Results

3.1. Temperature dependence of dye absorbance and fluorescence excitation ratios

The results of temperature scans of the fluorescence excitation spectra of RH421 and di-8-ANEPPS bound to dimyristoylphosphatidylcholine (DMPC) vesicles are shown in Fig. 2 and Fig. 3, respectively. The observed spectral shifts have been quantified via a ratiometric method, i.e., the ratio of the fluorescence intensities detected at two excitation wavelengths on the blue and red flanks of the excitation spectrum was measured as a function of the temperature. In the case of RH421, the excitation wavelengths chosen were 440 nm and 540 nm. In the case of di-8-ANEPPS, because its entire excitation spectrum is shifted approximately 20 nm to the blue relative to that of RH421, the excitation wavelengths chosen were 420 nm and 520 nm. For both dyes the ratio was measured at two different emission wavelengths: at 580 nm (close to the maximum of the emission spectrum) and at 670 nm (on the red edge of the emission spectrum).

The first point to note when examining Fig. 2 and Fig. 3, is that the measured value of the ratio depends strongly on the emission wavelength chosen. Irrespective of the temperature, for both dyes the fluorescence ratio is significantly higher at 580 nm than at 670 nm. This means that the excitation spectrum measured at 580 nm is blue shifted relative to that measured at an emission wavelength of 670 nm.

The second important point to note is the shape of the variation of the ratio with temperature. Curves of very different shape are observed at the two emission wavelengths. Before comparing the curves, however, one must remember that DMPC undergoes a gel-to-liquid-crystal phase transition at 23°C [25,32]. Below the phase transition temperature, i.e., in the gel phase, both dyes show an increase in their fluorescence ratios with increasing temperature at both emission wavelengths. Increases in the corresponding absorbance ratios (see Fig. 4) also occur. The observed changes can, therefore, be attributed to a process occurring in the ground state, presumably a change in the relative orientations of dye and lipid in the membrane.

Above the phase transition temperature, i.e., in the liquid crystalline phase, the behaviour of the fluorescence ratios depends strongly on the emission wavelength. At 580 nm both dyes show a significant drop in the fluorescence ratio with increasing temperature. Under these conditions both dyes are, therefore, quite sensitive to the viscosity of their surroundings. If the fluorescence is detected at 670 nm, however, no significant change in the fluorescence ratio is observed. For di-8-ANEPPS a drop in the absorbance ratio is observed above the phase transition temperature (see Fig. 4), indicating some ground state reorganization of dye and lipid. This is,

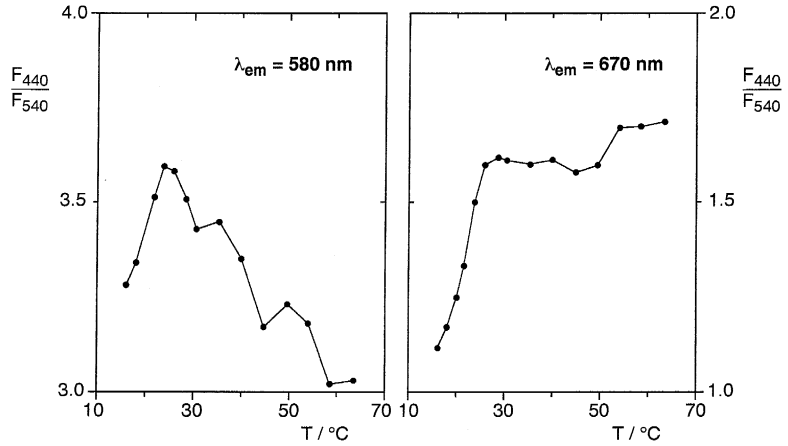

Fig. 2. Ratio of the RH421 fluorescence intensity produced by excitation at 440 nm to that produced by excitation at 540 nm, F_{440}/F_{540}, as a function of temperature, T, at emission wavelengths of 580 nm + OG570 cut-off filter (left) and 670 nm + RG645 cut-off filter (right); [RH421] = 4.3 μM, [DMPC] = 2900 μM, bandwidths = 5 nm.

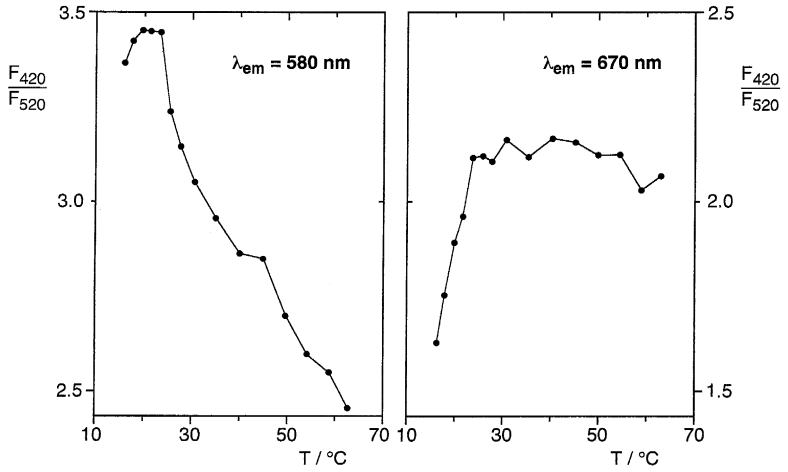

Fig. 3. Ratio of the di-8-ANEPPS fluorescence intensity produced by excitation at 420 nm to that produced by excitation at 520 nm, F_{420}/F_{520}, as a function of temperature, T, at emission wavelengths of 580 nm + OG570 cut-off filter (left) and 670 nm + RG645 cut-off filter (right); [di-8-ANEPPS] = 4.3 μM, [DMPC] = 2900 μM, bandwidths = 5 nm.

however, not apparent in the fluorescence data at 670 nm emission, indicating that the fluorescence detected under these conditions arises from a particular population of dye molecules which are insensitive to the reorganization. In contrast, in the absorbance measurements all dye molecules are observed and no selection is possible.

Fluorescence ratio measurements have also been performed for RH421 and di-8-ANEPPS bound to dioleoylphosphatidylcholine (DOPC) vesicles (see Fig. 5 and Fig. 6). This lipid is in the liquid crystalline phase across the whole temperature range of the experiments. As in the case of DMPC, it was found that the fluorescence ratio is independent of the membrane fluidity, if the fluorescence emission is detected at 670 nm. At 580 nm there is a significant decrease in the fluorescence ratio on increasing the temperature, although the effects are less than that observed in the case of DMPC. This could be explained by the greater fluidity of the DOPC membrane, which would presumably increase the rate of excited state relaxation of the dyes. The difference in

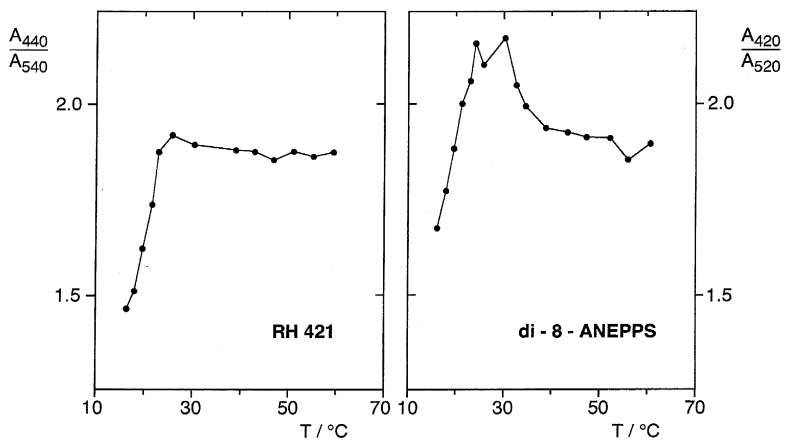

Fig. 4. Ratio of dye absorbance at two wavelengths as a function of temperature, T. Left: RH421, 4.3 μM, in the presence of 2900 μM of DMPC. The absorbance was measured at 440 nm and 540 nm. Right: di-8-ANEPPS, 4.3 μM, in the presence of 2200 μM of DMPC. The absorbance was measured at 420 nm and 520 nm. Bandwidth = 5 nm.

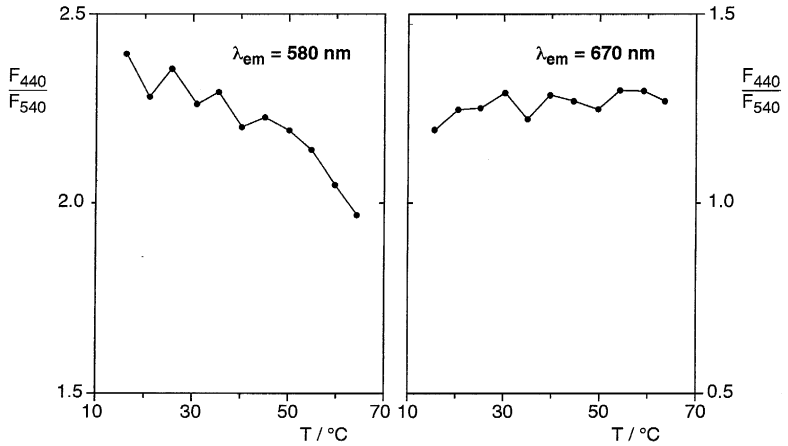

Fig. 5. Ratio of the RH421 fluorescence intensity produced by excitation at 440 nm to that produced by excitation at 540 nm, F_{440}/F_{540}, as a function of temperature, T, at emission wavelengths of 580 nm + OG570 cut-off filter (left) and 670 nm + RG645 cut-off filter (right); [RH421] = 4.3 μM, [DOPC] = 2250 μM, bandwidths = 5 nm.

the values of the fluorescence ratios obtained at the two wavelengths is also smaller for DOPC than for DMPC. This can similarly be attributed to the greater fluidity of the DOPC membrane.

In order to determine whether or not the temperature-induced changes of the fluorescence intensity ratios of RH421 and di-8-ANEPPS observed at 580 nm emission are specific to pure synthetic lipid vesicles, experiments have also been performed using vesicles made from a natural lipid mixture, i.e., egg phosphatidylcholine. The results obtained for both dyes were almost identical to those found for DOPC (see Fig. 5 and Fig. 6). The only difference was that the values of the fluorescence ratios obtained for egg phosphatidylcholine were approximately 10% higher those of DOPC. This could possibly be attributed to the presence of some saturated phosphatidylcholines such as DMPC in the egg phosphatidylcholine mixture. Therefore, the temperature-induced changes in the fluorescence ratios is a common property of both pure synthetic phosphatidylcholine and natural phosphatidylcholine mixtures.

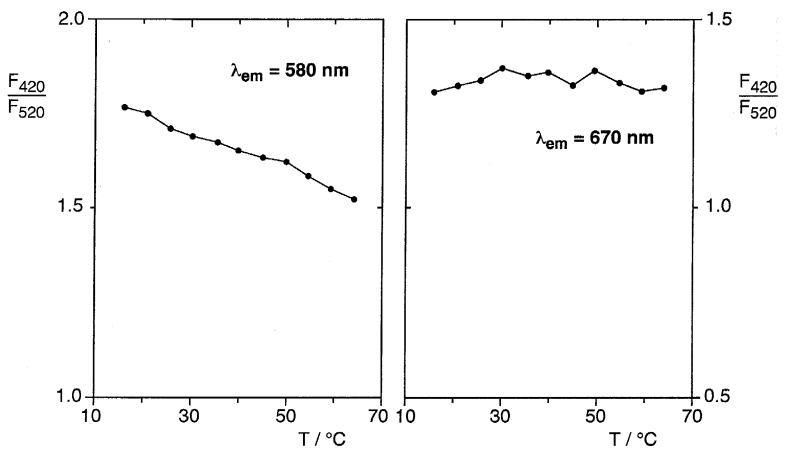

Fig. 6. Ratio of the di-8-ANEPPS fluorescence intensity produced by excitation at 420 nm to that produced by excitation at 520 nm, F_{420}/F_{520}, as a function of temperature, T, at emission wavelengths of 580 nm + OG570 cut-off filter (left) and 670 nm + RG645 cut-off filter (right); [di-8-ANEPPS] = 4.3 μM, [DOPC] = 2250 μM, bandwidths = 5 nm.

3.2. Binding of phloretin and 6-ketocholestanol to DMPC vesicles

In order to assess the relative sensitivities of RH421 and di-8-ANEPPS to changes in electrical potential, titrations have been carried out of membrane-bound dye with phloretin and 6-ketocholestanol. In accordance with the results of the temperature scans, viscosity effects have been excluded by measuring the fluorescence ratios at an emission wavelength of 670 nm.

Phloretin is a lipophilic dipolar substance that binds to lipid membranes and causes an increase in hydrophobic cation conductance and a decrease in hydrophobic anion conductance. This is true for both planar bilayers [31,33] and for unilamellar vesicles [34,35]. Andersen et al. [31] explained these changes in conductance by a decrease in the positive dipole potential of the membrane caused by phloretin inserting itself into the membrane such that its own dipole moment opposes the intrinsic dipole moment of the lipids. 6-Ketocholestanol, on the other hand, has been found to increase the positive dipole potential of phospholipid monolayers [36]. Franklin and Cafiso [35] found that it modifies the translocation rates of hydrophobic ions across the membranes of phospholipid vesicles, but in the opposite direction to phloretin. They, therefore, concluded that 6-ketocholestanol increases the magnitude of the dipole potential of phospholipid bilayers. Based on these results, Gross et al. [18] used phloretin and 6-ketocholestanol as tools to conveniently decrease and increase the membrane dipole potential, respectively, and so test the feasibility of di-8-ANEPPS as a probe of dipole potential. In the present paper we have used the same approach to compare the sensitivities of RH421 and di-8-ANEPPS. Gross et al. [18] attribute the spectral responses of the dyes to phloretin and 6-ketocholestanol to the change in dipole potential alone and exclude any effects due to complexation of dye with the two substrates.

The effects of increasing concentrations of phloretin and 6-ketocholestanol on the fluorescence ratio, R, of membrane-bound RH421 and di-8-ANEPPS are shown in Fig. 7 and Fig. 8. In Fig. 7 it can be seen that the binding of phloretin to the membrane can be well described by a saturable binding model. This is in agreement

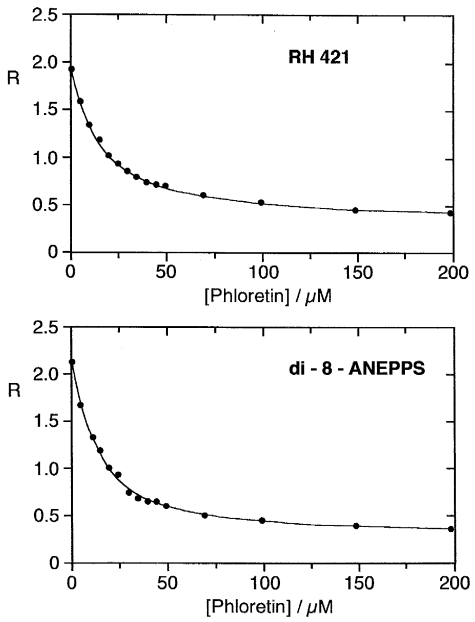

Fig. 7. Fluorescence intensity ratios, R, of 4.3 μM RH421 (top) and 4.3 μM di-8-ANEPPS (bottom) in the presence of 200 μM of DMPC as a function of the phloretin concentration. In both cases the fluorescence emission was observed at 670 nm (+RG645 cut-off filter). In the case of RH421, R represents the ratio of the fluorescence intensity produced by excitation at 440 nm to that produced by excitation at 540 nm. In the case of di-8-ANEPPS the excitation wavelengths were 420 nm and 520 nm. $T = 30$°C, bandwidths = 5 nm. The solid lines represent fits of the data to Eq. (7) and Eq. (8).

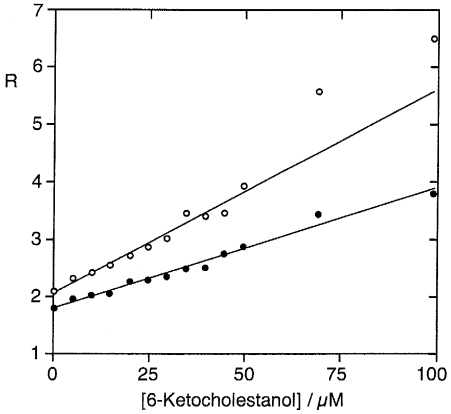

Fig. 8. Fluorescence intensity ratios, R, of 4.3 μM RH421 (●) and 4.3 μM di-8-ANEPPS (○) in the presence of 200 μM of DMPC as a function of the 6-ketocholestanol concentration. The excitation and emission wavelengths were as in Fig. 5. $T = 30$°C, bandwidths = 5 nm.

with previous studies of phloretin binding to lipid monolayers [37], planar lipid bilayers [38,39], unilamellar phosphatidylcholine vesicles [40,41] and red blood cell ghosts [42], which have all been carried out by very different experimental methods to that employed here. Fitting the data obtained to Eqs. (7) and (8) in Section 2 yields an apparent binding constant, K, of phloretin to the membrane of $1.25\ (\pm 0.10) \cdot 10^5\ M^{-1}$ when RH421 was used as the probe and $1.61\ (\pm 0.25) \cdot 10^5\ M^{-1}$ when di-8-ANEPPS was used. The number of binding sites per lipid molecule, n, were determined to be $0.046\ (\pm 0.009)$ using RH421 and $0.043\ (\pm 0.014)$ using di-8-ANEPPS. Titrations were also carried out at pH 5 (data not shown) and the results obtained were fitted to Eqs. (2) and (8). Within experimental error the values of K and n determined were identical to those at pH 7.

The values of K and n determined here can be compared to values reported in previous studies. From spectrophotometric titrations of the phloretin absorbance as a function of the lipid concentration, Verkman and Solomon [40] determined the dissociation constant of phloretin with egg phosphatidylcholine vesicles to be 8.0 μM ($K = 1.25 \cdot 10^5\ M^{-1}$). Verkman [41] made use of the fluorescence quenching of membrane-bound probes by phloretin and determined a dissociation constant of 9 μM ($K = 1.1 \cdot 10^5\ M^{-1}$). Jennings and Solomon [42] reported a dissociation constant of phloretin with red blood cell ghosts of 0.44 μM ($K = 2.3 \cdot 10^4\ M^{-1}$). From temperature-jump kinetic studies of the binding of phloretin to planar lipid bilayers, Awiszus and Stark [39] determined a dissociation constant of 8 μM ($K = 1.25 \cdot 10^5\ M^{-1}$). Therefore, apart from the measurements of Jennings and Solomon [42] on red cell ghosts, the values of K determined here are in good agreement with those determined by other methods. The significantly different value found for red cell ghosts may be due to a different lipid constitution of the membrane.

The values of n calculated here of around 0.045 binding sites per lipid molecule corresponds to 22 lipid molecules per phloretin binding site. Verkman and Solomon [40] and Verkman [41] reported 4 lipid molecules per binding site. Awiszus and Stark [39] determined a maximum density of phloretin in the membrane of $2.2 \cdot 10^{13}$ molecules per cm^2. Comparing this to the typical density of lipid molecules in a phosphatidylcholine membrane of $1.5 \cdot 10^{14}$ per cm^2 [32,43] yields a value of 7 lipid molecules per binding site. The number of lipid molecules per binding site found here is, therefore, somewhat higher than previously reported values. A possible explanation might be an interaction between phloretin and the probes in the membrane phase. Titrations at lower probe concentrations could show whether this is actually the case.

In the case of the binding of 6-ketocholestanol to lipid vesicles (see Fig. 8), no evidence of saturation of the membrane could be found in the concentration range studied. R increases linearly with the concentration of 6-ketocholestanol. At concentrations above 100 μM precipitation occurs in the aqueous phase. The measurements performed using di-8-ANEPPS showed a positive deviation from linearity at high concentrations of

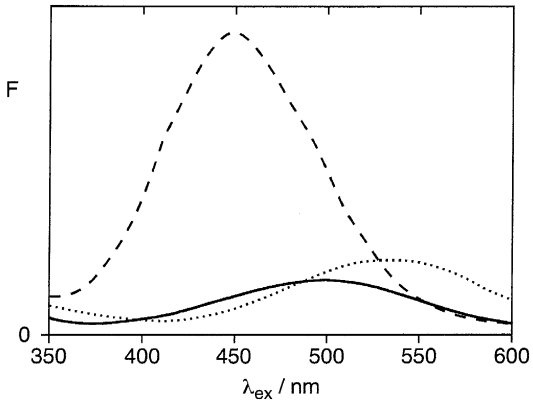

Fig. 9. Corrected fluorescence excitation spectra of 4.3 μM RH421 in aqueous solution alone (solid curve), in the presence of 495 μM of phloretin (dotted curve) and in the presence of 30 μM of 6-ketocholestanol (dashed curve). $\lambda_{em} = 670$ nm (+RG645 cut-off filter), $T = 30$°C, excitation bandwidth = 5 nm, emission bandwidth = 5 nm.

6-ketocholestanol. At such high concentrations it is feasible that 6-ketocholestanol may perturb the membrane structure.

The results in Fig. 7 and Fig. 8 show that in DMPC membranes di-8-ANEPPS is more sensitive than RH421 towards both phloretin and 6-ketocholestanol. The maximum change in R induced by phloretin is only 5% higher for di-8-ANEPPS than RH421. Based on the slopes of the plots in Fig. 8, however, di-8-ANEPPS is significantly more sensitive than RH421 towards 6-ketocholestanol. The slope of R against 6-ketocholestanol concentration is 67% greater than that found for RH421.

3.3. Interaction of phloretin and 6-ketocholestanol with dye in aqueous solution

Phloretin and 6-ketocholestanol cause red and blue shifts, respectively, of the fluorescence excitation spectra of RH421 (see Fig. 9) and di-8-ANEPPS in aqueous solution. Both substances also cause significant increases in the fluorescence intensity. The fluorescence intensity increase is much greater on the addition of 6-keto-cholestanol than phloretin and the effects observed are even greater for di-8-ANEPPS than for RH421. In the case of RH421 the addition of 6-ketocholestanol is accompanied by a shift of the fluorescence emission maximum from its normal value in water of around 650 nm [27] to a value of approximately 580 nm. The effects of phloretin and 6-ketocholestanol on the fluorescence intensity could be partly explained by the breaking up of dye aggregates in the aqueous solution [19,44]. Additionally there may be an effect on the excited state relaxation process of the dyes.

The magnitudes of the excitation shifts increase with increasing dye concentration (see Fig. 10). This could be explained by a change in stoichiometry between the dye and the two substrates. At low dye concentrations a single dye molecule would be surrounded by several phloretin or 6-ketocholestanol molecules. On increasing the dye concentration, the equilibrium would shift in the favour of 1:1 dye–substrate complexes. In the case of both phloretin and 6-ketocholestanol, the magnitude of the shift appears to be greater for 1:1 complexes than for those of higher stoichiometry. If the shifts are attributed to the local electric fields induced by the substrates, it would seem that the field strength induced by a single substrate molecule is greater than that induced by a number of substrate molecules. This would be expected if the substrate molecules do not all have the same orientation with respect to the dye, e.g. as in a micellar structure, so that the electric field lines from the individual molecules interfere.

In ethanolic solution, neither phloretin nor 6-ketocholestanol had any effect on the dyes excitation spectra. It seems, therefore, that hydrophobic interactions are likely to be a driving force for the association reaction. This

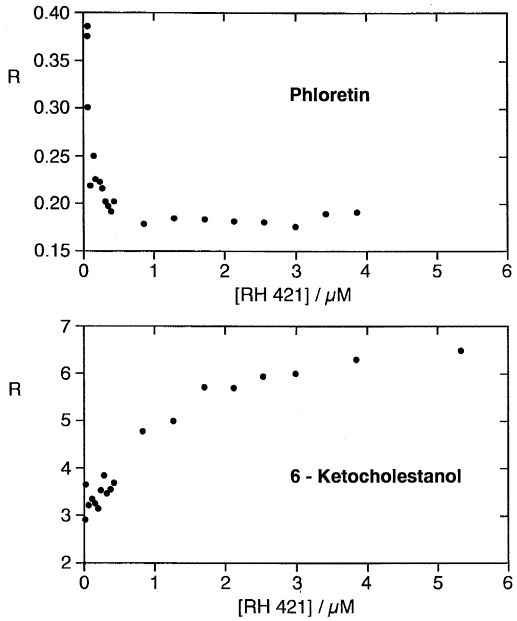

Fig. 10. Fluorescence intensity ratio, R, of RH421 in aqueous solution in the presence of 495 μM phloretin (above) and 30 μM 6-ketocholestanol (below) as a function of the RH421 concentration. $\lambda_{em} = 670$ nm (+RG645 cut-off filter), $T = 30$°C, excitation bandwidth = 5 nm, emission bandwidth = 20 nm.

is consistent with the attribution of the fluorescence increases of the dyes to the dissolution of dye aggregates, since it is known that the dyes aggregate much more strongly in water compared to organic solvents [16,27].

3.4. Effect of dye–dye interactions on fluorescence excitation ratios

It has recently been suggested by Malkov and Sokolov [28] that RH421 and related dyes increase the membrane dipole potential. If one looks at the structure of the dyes (see Fig. 1), this is entirely feasible, since one would expect the dyes to bind based on electrostatic considerations such that the localized negative charge on the sulfonate group is in the adjacent aqueous phase and the delocalized positive charge on the aromatic chromophore is in the membrane phase. If the fluorescence excitation spectrum of bound dye is to be used to probe the dipole potential, it is, therefore, necessary to exclude any spectral shifts caused by the electric field induced by adjacent dye molecules. In the following we investigate the effect of dye surface density in the membrane on the fluorescence excitation spectrum.

In Fig. 11 it can be seen that at constant dye concentration both dyes show a decrease in R on increasing the lipid concentration, although the effect is significantly greater for RH421 than for di-8-ANEPPS. Since the lipid concentration is always far in excess of the dye concentration, almost all of the dye is in the membrane phase and the increase in R at low lipid concentrations can confidently be attributed to dye–dye interactions in the membrane. Considering the results of Malkov and Sokolov [28], a possible explanation for this effect is an electrostatic interaction between the dye molecules caused by their effect on the dipole potential. The fact that the interaction causes an increase in R, i.e., a blue shift of the excitation spectrum, as observed in the case of 6-ketocholestanol (see Fig. 8), is consistent with a dye-induced increase in the dipole potential.

Similar shifts in the excitation spectrum have previously been observed for RH421 [27] and the related dye RH160 [13] bound to Na^+,K^+-ATPase-containing membrane fragments. There the shifts were interpreted as being due to dye aggregation within the membrane [27] or to a protein–dye interaction [13]. In order to test

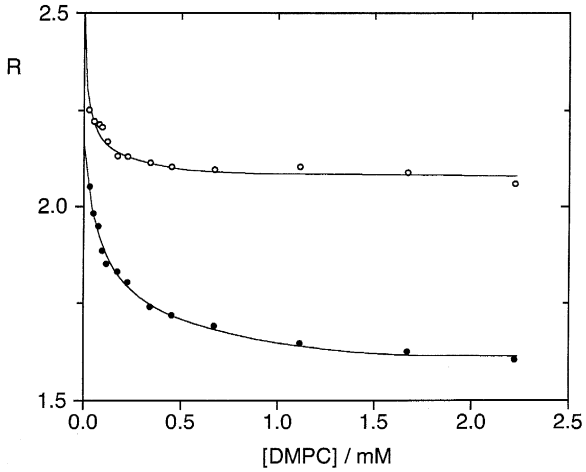

Fig. 11. Fluorescence intensity ratio, R, of 4.3 μM RH421 (●) and 4.3 μM di-8-ANEPPS (○) as a function of the DMPC concentration. The excitation and emission wavelengths were as in Fig. 5. $T = 30$°C, bandwidths = 5 nm. The solid lines represent fits of the data to Eq. (A5).

whether or not dye aggregation could be occurring here, we have analyzed the curves in Fig. 11 in terms of the surface density of dye and in terms of a dye monomer/dimer equilibrium (see Appendix A).

At this stage it is not possible based on the results presented here to distinguish between a weak dye dimerization in the membrane phase and an electrostatic interaction coming about merely by the statistical distribution of dye molecules over the surface. In the light of the results of Malkov and Sokolov [28], however, showing that styryl dyes increase the dipole potential, an electrostatic interaction may be more likely.

From the curves in Fig. 11 it can be seen that for RH421 significant dye–dye interactions are already observed at a lipid concentration of around 0.5 mM, which corresponds to a lipid/dye molar ratio in the membrane of 117:1. Therefore, if RH421 is to be used as a probe of the dipole potential, simultaneously avoiding any effects due to dye–dye interactions, there should be at least a 200-fold excess of lipid molecules over dye in the membrane. In the case of di-8-ANEPPS, the observed shifts are smaller and the interaction first becomes apparent at lower lipid concentrations. If the interaction is purely electrostatic in origin, this could be explained by a lower dipole moment of di-8-ANEPPS compared to RH421 or by a different depth of insertion into the membrane, which would cause it to experience a different effective dielectric constant of its surroundings. Because the effects of dye–dye interactions are smaller for di-8-ANEPPS, a lower lipid/dye molar ratio could be used without observing any effects due to the dye, but an excess of lipid molecules over dye of at least 100-fold should in any case be employed.

4. Discussion

The fluorescent styrylpyridinium dyes, such as RH421 [19] and di-8-ANEPPS [18] have recently been suggested as probes of the membrane dipole potential. Gross et al. [18] proposed the use of a dual wavelength excitation ratiometric fluorescence method, which was originally introduced by Montana et al. [20] for measuring the transmembrane potential. If this method is to be applicable it must meet certain requirements. Firstly, the dyes should respond to the dipole potential alone and not to changes in other membrane properties such as the fluidity. Secondly, the dyes themselves should not modify the dipole potential.

Gross et al. [18] claim that the fluorescence ratio, R, of di-8-ANEPPS is not sensitive to membrane microviscosity. Based on the experiments reported here using DMPC and DOPC vesicles, this is not valid for all

lipids and all conditions. The value of R is only insensitive to membrane viscosity under specific experimental conditions. It has been found that the choice of the emission wavelength is critical in excluding viscosity effects. Both RH421 and di-8-ANEPPS show a strong dependence of R on the membrane fluidity (varied by changing the temperature) when the fluorescence is detected close to the emission maximum, i.e., around 580 nm (see Fig. 2, Fig. 3, Fig. 5 and Fig. 6). Below the DMPC phase transition temperature of 23°C significant changes in the value of R are observed, which can be attributed to changes in the relative orientations of lipid and dye in the ground state (see Fig. 4). The value of R is only insensitive to membrane fluidity above the phase transition temperature and only if the fluorescence is detected at the red edge of the emission spectrum, i.e., at 670 nm.

Detection at 670 nm selects a particular population of dye molecules whose fluorescence does not depend on the fluidity of their surroundings. This can partly be explained by a relatively slow excited state relaxation of membrane bound dye molecules [17,25,26], whose rate depends on the membrane fluidity. Red edge detection, however, selects only those dye molecules which have already reached the fully relaxed excited state, so that the measured excitation spectrum is no longer dependent on the fluidity. A further contributing factor may be ground state heterogeneity of the membrane-bound dye molecules. The fluorescence detected at 670 nm may arise largely from dye molecules which at the moment of absorption of a photon happen to be in a ground state conformation (this includes dye and its solvent/lipid shell) which corresponds closely to that of the relaxed excited state.

Comparison of the results obtained with DMPC and DOPC vesicles indicate that the dyes are less sensitive to temperature when bound to DOPC than DMPC. This can be explained by the higher fluidity of the DOPC membrane, which could lead to a more rapid excited state relaxation. In biological membranes, wide variations in the degree of fluidity are found. In some cases, particularly when a high concentration of protein is present, biological membranes can be even more rigid than DMPC. For example, the rotational diffusion constant of RH421 bound to Na^+,K^+-ATPase-containing membrane fragments from rabbit kidney is less than half that of the same dye when bound to DMPC in the liquid crystalline state [17]. Therefore, the avoidance of membrane fluidity effects is an important consideration, both in natural and model membranes.

Now let us compare the R values obtained at 670 nm for the two lipids. In the case of RH421, R has a value of about 1.6 for DMPC above the phase transition temperature and 1.25 for DOPC. In the case of di-8-ANEPPS, R has a value of about 2.1 for DMPC above the phase transition temperature and 1.3 for DOPC. Therefore, in both cases the value of R is significantly lower for DOPC than for DMPC. Since the addition of phloretin, which has been proposed to decrease the dipole potential, also decreases the value of R, this would suggest that DOPC has a significantly lower dipole potential than DMPC. Such a possibility has previously been suggested to explain the significantly lower pK_a of RH421 bound to DMPC vesicles compared to DOPC [19]. This may have important physiological consequences, since variation in the lipid content of biological membranes could be expected to modify the dipole potential, which may then have a direct electrical influence on the kinetics of ion-translocating membrane proteins. A systematic study of the effect of lipid structure on the magnitude of the dipole potential is presently under way.

In dimyristoylphosphatidylcholine vesicles, di-8-ANEPPS is slightly more sensitive than RH421 to the addition of the lipophilic dipolar substrates phloretin and 6-ketocholestanol (see Fig. 7 and Fig. 8). These shifts were interpreted by Gross et al. [18] as indicating increases and decreases in the membrane dipole potential. Here it has been found that similar shifts are observed in aqueous solution (see Fig. 9). Therefore, in aqueous solution a direct interaction of phloretin and 6-ketocholestanol with the dyes must be occurring. This does not necessarily imply that a direct interaction occurs in membranes. The reason for the spectral shifts in water is not clear at this stage. A possibility is that the local electric field induced by phloretin and 6-ketocholestanol in the neighbourhood of the dyes may cause a change in the electronic distribution of the chromophore and perhaps simultaneously modify the solvation of the dye, i.e., the strength of interaction of water with the positively charged pyridinium moiety. In the membrane similar effects may be occurring, particularly as it has been suggested that the dipole potential may arise partly from oriented water molecules in the interface [45,46].

In DMPC vesicles, both RH421 and di-8-ANEPPS have been found to induce blue shifts of the fluorescence

excitation spectrum at high dye:lipid ratios (see Fig. 11). Similar shifts were previously observed for RH421 in Na^+,K^+-ATPase-containing membrane fragments [27]. Fedosova et al. [13] also observed shifts of the related dye RH160 depending on the protein:lipid ratio in the membrane. These shifts could be explained by a dye-induced increase in the membrane dipole potential, since the shift is in the same direction as for 6-ketocholestanol, which has also been suggested to increase the dipole potential [35,36]. This is furthermore consistent with the results of Malkov and Sokolov [28], who showed that the binding of RH421 to planar lipid membranes leads to a significant acceleration of the transport of hydrophobic anions through the membrane. A dye-induced increase in dipole potential may also be able to explain the reported inhibition of ATP hydrolysis by the Na^+,K^+-ATPase at RH421 concentrations in the micromolar range (see Fig. 5 of [14]). An inhibition of ATP hydrolysis accompanying the uncoupled Na^+-efflux mode of action of the Na^+,K^+-ATPase has been observed on the addition of the positively charged hydrophobic ion tetraphenylphosphonium (TPP^+) [47]. Cornelius [47] attributed the effect of TPP^+ to an increase in the positive potential inside the membrane, which inhibits a rate-determining charge-translocating step of the uncoupled Na^+-efflux pump cycle of the Na^+,K^+-ATPase, probably the dephosphorylation step. Furthermore, the binding affinity of cytoplasmic Na^+ ions to the protein was found to decrease on the addition of TPP^+ [47,48]. Neither of these reaction steps are, however, able to explain the inhibition by RH421, which was measured in the presence of both Na^+ and K^+ ions, because under these conditions neither dephosphorylation nor cytoplasmic Na^+ ion binding are generally regarded to be rate limiting [49]. A more likely explanation is an effect of RH421 on the Na^+ translocation process, i.e., the associated conformational change of the protein or the release of Na^+ ions from their binding sites. If it is true, that the dipole potential affects the rate of Na^+ translocation, it means that the portion of the protein in which the translocation reaction occurs must be so narrow that it is not sufficiently electrically shielded by protein mass from the surrounding lipid and that the reaction must involve a movement of charge across a major proportion of the dipole potential gradient [50].

If one wishes to use RH421 or di-8-ANEPPS as probes of the dipole potential or of the kinetics of ion pumps, it is necessary to avoid changes in the dipole potential from the dyes themselves. The changes in R shown in Fig. 11 allow one to estimate the molar lipid/dye excess necessary for this. In the case of RH421, which has a greater influence on the excitation spectrum than di-8-ANEPPS, a 200-fold excess of lipid molecules to dye in the membrane is necessary. In the case of di-8-ANEPPS, a 100-fold excess would be sufficient. In the light of its greater sensitivity to phloretin and 6-ketocholestanol as well as its smaller effect on its own excitation spectrum, it would seem that, at least in the case of DMPC membranes, di-8-ANEPPS is to be preferred over RH421 as a probe of the dipole potential.

Acknowledgements

We thank Dr. Klaus Fendler, Dr. Shab Ladha and Mr. Tiemen van der Heide for valuable discussions and suggestions. For his interest and support of this work we thank Prof. Dr. Ernst Bamberg. We acknowledge with gratitude financial support from the Max-Planck-Gesellschaft.

Appendix A. Analysis of dye-induced fluorescence shifts

At excess concentrations of lipid, the moles of dye bound per volume of suspension, c^*_{DL}, is given by [25],

$$c^*_{DL} = \left(\frac{nKc^*_L}{1 + nKc^*_L} \right) c^*_D \tag{A1}$$

where c^*_D is the total concentration of dye. n, K and c^*_L are as defined in Section 2. The surface area occupied

by one phosphatidylcholine molecule in the liquid crystalline phase is approximately $65 \cdot 10^{-20}/\mathrm{m}^2$ [32,43]. The total surface area of lipid, A, in m^2 per dm^3 of suspension is, therefore, given by

$$A = 65 \cdot 10^{-20} \cdot N_A c_L^* \tag{A2}$$

where N_A is Avogadro's constant. The surface density of dye, S, in mol m^{-2} is then given by dividing Eq. (A1) by Eq. (A2):

$$S = \frac{c_D^*}{3.914 \cdot 10^5} \cdot \frac{nK}{1 + nKc_L^*} \tag{A3}$$

If one assumes that the dye–dye interaction comes about merely by the proximity of neighbouring dye molecules distributed evenly over the surface, then the value of R would be expected to vary according to the surface density of dye, S. Assuming initially a linear relationship between R and S, the value of R could then be fitted to the total lipid concentration, c_L^*, by the following equation:

$$R = R_0 + k \cdot \frac{c_D^*}{3.914 \cdot 10^5} \cdot \frac{nK}{1 + nKc_L^*} \tag{A4}$$

where R_0 is the value of R at infinitely high lipid concentrations such that no dye–dye interactions are occurring and k is a constant of proportionality. The values of the binding affinities, nK, of RH421 and di-8-ANEPPS to DMPC vesicles at 30°C have been determined by titrating dye with vesicles and measuring the fluorescence, as described in Zouni et al. [25] to be $2.2\ (\pm 0.5) \cdot 10^4\ \mathrm{M}^{-1}$ for RH421 and $5.3\ (\pm 1.2) \cdot 10^4\ \mathrm{M}^{-1}$ for di-8-ANEPPS. Using these values it is possible to fit the data in Fig. 11 to Eq. (A4). It was found that Eq. (A4) was able to explain the general shape of the dependence of R on c_L^*. There were, however, some systematic positive and negative deviations of the fitted curve from the experimental data. In order to obtain a better fit, Eq. (A4) has been modified to incorporate a phenomenological power dependence of R on the surface density:

$$R = R_0 + k\left[\frac{c_D^*}{3.914 \cdot 10^5} \cdot \frac{nK}{1 + nKc_L^*}\right]^x \tag{A5}$$

Eq. (A5) provides a good fit of the data in Fig. 11. For RH421 the values of the various parameters calculated from the fits were: $R_0 = 1.48\ (\pm 0.01)$, $k = 4.5\ (\pm 0.8) \cdot 10^2$ and $x = 0.43\ (\pm 0.1)$. In the case of di-8-ANEPPS, $R_0 = 2.066\ (\pm 0.008)$, $k = 4\ (\pm 1) \cdot 10^3$ and $x = 0.66\ (\pm 0.02)$.

The fact that the dye-induced shifts in the fluorescence excitation spectrum can be explained by the statistical distribution of dye within the membrane would tend to support the argument that the shifts arise from an electrostatic interaction, e.g., from a dye-induced increase in dipole potential. In this case the value of R would increase with increasing dipole potential and the physical significance of k can be discussed further. The value of k would then depend on the component of the dye dipole moment which is perpendicular to the membrane-solution interface, μ, and the dielectric constant of the membrane at the position where the dye dipole is located, ϵ, [28], i.e., k would increase with increasing μ and decrease with increasing ϵ. A later electrical calibration of the dyes could, however, allow a more exact relationship to be derived.

An alternative method to fit the data in Fig. 11 could be obtained by making the value of k in Eq. (A4) a function of the surface density. In order to obtain a suitable fit, k must decrease with increasing surface density. This would mean that μ decreases with increasing surface density and/or ϵ increases. Both situations could be explained by a reorientation of dye towards the membrane–solution interface with increasing surface density. This method of fitting the data would seem to be more physically relevant than the phenomonological description of Eq. (A5). However, the exact mathematical dependence of k on the dye surface density is not clear at this stage.

The data in Fig. 11 can, however, equally well be described by a relatively weak dimerization of dye in the membrane phase. The dimerization constant, K_D, is defined as follows,

$$K_D = \frac{[D]}{[M]^2} \tag{A6}$$

where [D] and [M] are the surface concentrations of dye dimer and monomer, respectively. The value of [M] can be calculated from the total surface density of dye, S (given by Eq. (A3)), by

$$[M] = \frac{-1 + \sqrt{1 + 8K_D S}}{4K_D} \tag{A7}$$

The value of R would in this case vary between the limiting values of R_1 for dye monomers and R_2 for dye dimers and would be given by

$$R = R_1 \cdot \frac{[M]}{S} + R_2 \cdot \frac{2K_D[M]^2}{S} \tag{A8}$$

Fitting the experimental data to Eq. (A7) and Eq. (A8) yields the following values of the parameters. For RH421: $R_1 = 1.59\ (\pm 0.01)$, $R_2 = 2.8\ (\pm 0.1)$ and $K_D = 2.9\ (\pm 0.7) \cdot 10^6\ m^2\ mol^{-1}$. For di-8-ANEPPS: $R_1 = 2.06\ (\pm 0.06)$, $R_2 = 2.48\ (\pm 0.06)$ and $K_D = 2.7\ (\pm 1.5) \cdot 10^6\ m^2\ mol^{-1}$. The reciprocal of the K_D values indicate the surface dye concentration necessary for half of the dye molecules to be in the dimer form. Taking a value of $3 \cdot 10^6\ m^2\ mol^{-1}$ for K_D for both dyes, this corresponds to a surface concentration of $3.3 \cdot 10^{-7}$ mol m^{-2}, i.e., $2 \cdot 10^{17}$ molecules m^{-2}. This value can be compared to the surface concentration of phosphatidylcholine molecules in a pure lipid membrane of $1.5 \cdot 10^{18}$ molecules m^{-2}. The dye surface concentration necessary for 50% dimerization would, thus, be approximately one tenth of the lipid concentration. This indicates that, if the shifts of the excitation spectra are attributed to dye dimerization, the forces of attraction between the dye molecules must be relatively weak.

References

[1] Grinvald, A., Hildesheim, R., Farber, I.C. and Anglister, L. (1982) Biophys. J. 39, 301–308.
[2] Grinvald, A., Fine, A., Farber, I.C. and Hildesheim, R. (1983) Biophys. J. 42, 195–198.
[3] Hassner, A., Birnbaum, D. and Loew, L.M. (1984) J. Org. Chem. 49, 2546–2551.
[4] Fluhler, E., Burnham, V.G. and Loew, L.M. (1985) Biochem. 24, 5749–5755.
[5] Bedlack, R.S. Jr., Wei, M.-D. and Loew, L.M. (1992) Neuron 9, 393–403.
[6] Grinvald, A., Frostig, R.D., Lieke, E. and Hildesheim, R. (1988) Physiol. Rev. 68, 1285–1366.
[7] Loew, L.M. (1994) Neuroprotocols 5, 72–79.
[8] Fromherz, P. and Müller, C.O. (1994) Proc. Natl. Acad. Sci. USA 91, 4604–4608.
[9] Gogan, P., Schmiedel-Jakob, I., Chitti, Y. and Tyc-Dumont, S. (1995) Biophys. J. 69, 299–310.
[10] Klodos, I. and Forbush, B. III (1988) J. Gen. Physiol. 92, 46a.
[11] Pratap, P.R. and Robinson, J.D. (1993) Biochim. Biophys. Acta 1151, 89–98.
[12] Heyse, S., Wuddel, I., Apell, H.-J. and Stürmer, W. (1994) J. Gen. Physiol. 104, 197–240.
[13] Fedosova, N.U., Cornelius, F. and Klodos, I. (1995) Biochem. 34, 16806–16814.
[14] Frank, J., Zouni, A., van Hoek, A., Visser, A.J.W.G. and Clarke, R.J. (1996) Biochim. Biophys. Acta 1280, 51–64.
[15] Bühler, R., Stürmer, W., Apell, H.-J. and Läuger, P. (1991) J. Membr. Biol. 121, 141–161.
[16] Clarke, R.J., Zouni, A. and Holzwarth, J.F. (1995) Biophys. J. 68, 1406–1415.
[17] Visser, N.V., Van Hoek, A., Visser, A.J.W.G., Frank, J., Apell, H.-J. and Clarke, R.J. (1995) Biochem. 34, 11777–11784.
[18] Gross, E., Bedlack, R.S. Jr. and Loew, L.M. (1994) Biophys. J. 67, 208–216.
[19] Zouni, A., Clarke, R.J. and Holzwarth, J.F. (1994) J. Phys. Chem. 98, 1732–1738.
[20] Montana, V., Farkas, D.L. and Loew, L.M. (1989) Biochem. 28, 4536–4539.
[21] Grynkiewicz, G., Poenie, M. and Tsien, R.Y. (1985) J. Biol. Chem. 260, 3440–3450.

[22] Loew, L.M., Cohen, L.B., Dix, J., Fluhler, E.N., Montana, V., Salama, G. and Jian-young, W. (1992) J. Membr. Biol. 130, 1–10.
[23] Bedlack, R.S. Jr., Wei, M.-D., Fox, S.H., Gross, E. and Loew, L.M. (1994) Neuron 13, 1187–1193.
[24] Schulz, S. and Apell, H.-J. (1995) Eur. Biophys. J. 23, 413–421.
[25] Zouni, A., Clarke, R.J., Visser, A.J.W.G., Visser, N.V. and Holzwarth, J.F. (1993) Biochim. Biophys. Acta 1153, 203–212.
[26] Visser, N.V., Van Hoek, A., Visser, A.J.W.G., Clarke, R.J. and Holzwarth, J.F. (1994) Chem. Phys. Lett. 231, 551–560.
[27] Clarke, R.J., Schrimpf, P. and Schöneich, M. (1992) Biochim. Biophys. Acta 1112, 142–152.
[28] Malkov, D.Y. and Sokolov, V.S. (1996) Biochim. Biophys. Acta 1278, 197–204.
[29] Bashford, C.L. and Smith, J.C. (1979) Biophys. J. 25, 81–85.
[30] Le Fevre, P.G. and Marshall, J.K. (1959) J. Biol. Chem. 234, 3022–3026.
[31] Andersen, O.S., Finkelstein, A., Katz, I. and Cass, A. (1976) J. Gen. Physiol. 67, 749–771.
[32] Cevc, G. and Marsh, D. (1987) Phospholipid Bilayers. Physical Principles and Models, pp. 242, 334, Wiley, New York.
[33] Melnik, E., Latorre, R., Hall, J.E. and Tosteson, D.C. (1977) J. Gen. Physiol. 69, 243–257.
[34] Perkins, W.R. and Cafiso, D. (1987) J. Membr. Biol. 96, 165–173.
[35] Franklin, J.C. and Cafiso, D.S. (1993) Biophys. J. 65, 289–299.
[36] Simon, S.A., McIntosh, T.J., Magid, A.D. and Needham, D. (1992) Biophys. J. 61, 786–799.
[37] Reyes, J., Greco, R., Motais, R. and Latorre, R. (1983) J. Membr. Biol. 72, 93–103.
[38] De Levie, R., Rangarajan, S.K., Seelig, P.F. and Andersen, O.S. (1979) Biophys. J. 25, 295–300.
[39] Awiszus, R. and Stark, G. (1988) Eur. Biophys. J. 15, 321–328.
[40] Verkman, A.S. and Solomon, A.K. (1980) J. Gen. Physiol. 75, 673–692.
[41] Verkman, A.S. (1980) Biochim. Biophys. Acta 599, 370–379.
[42] Jennings, M.L. and Solomon, A.K. (1976) J. Gen. Physiol. 67, 381–397.
[43] Marsh, D. (1993) in Biomembranes. Physical aspects (Shinitzky, M., ed.), p. 12, VCH Verlag, Weinheim, Germany.
[44] Lojewska, Z. and Loew, L.M. (1987) Biochim. Biophys. Acta 899, 104–112.
[45] Gawrisch, K., Ruston, D., Zimmerberg, J., Parsegian, V.A., Rand, R.P. and Fuller, N. (1992) Biophys. J. 61, 1213–1223.
[46] Zheng, C. and Vanderkooi, G. (1992) Biophys. J. 63, 935–941.
[47] Cornelius, F. (1995) Biochim. Biophys. Acta 1235, 183–196.
[48] Stürmer, W., Bühler, R., Apell, H.-J. and Läuger, P. (1991) J. Membr. Biol. 121, 163–176.
[49] Forbush B. III and Klodos, I. (1991) in The Sodium Pump: Structure, Mechanism, and Regulation (Kaplan, J.H. and DeWeer, P., eds.), pp. 211–225, Rockefeller University Press, New York.
[50] Jordan, P.C. (1983) Biophys. J. 41, 189–195.